# The most stable transition state complexes of the aminotoluene molecule

B. Eren[1], Y. Y. Gurkan[2]*

*[1]Namik Kemal University, Faculty of Agriculture, Tekirdag / Turkey*
*[2]Namik Kemal University, Department of Chemistry, Tekirdag / Turkey*

In this study the most probable reaction paths of ATnm, OATnm, MATnm, PATnm, NMATo and NMATm transition states with OH radicals have been analyzed. The optimized geometry was calculated via Gauss View 5. Subsequently, the lowest energy level was found by geometric optimization via the Gaussian 09 programme. The geometrical structure analysis and bond lengths were also calculated. This study aims to determine the most probable path for the product distribution of transition state complexes and OH radical interaction in the gas phase and aqueous media. Quantum mechanical methods were used to indicate the impact of the reaction rate over the primary intermediate, hydroxylated intermediate and finally the impact of water solvent. With the aim to determine the intermediates occurring at the reaction of transition state complexes degradation, the geometric optimization of the reactant and transition state complexes were realized through semiempirical AM1 and PM3, ab initio Hartree-Fock HF/3-21G, HF/6-31G* and Density Functional Theory (DFT) methods. Determining the most appropriate method and the reliability of the method are compared and evaluated theoretically. Based on the Quantum mechanical calculation, all the probable rate constants of reaction paths were calculated by using Transition State Theory (TST). In order to determine the transition state of the reaction, C-O bonds were taken as a reference. Activation energy for probable reaction paths of all transition state complexes, and their most stable state were calculated from the thermodynamic perspective for the gas phase and aqueous media. The impact of water solvent was investigated by using COSMO as the solvation model.

Keywords: Aminotoluene, AM1, PM3, HF, TST.

## INTRODUCTION

Volatile aromatic compounds constitute a major part of air and water contaminants. They are mainly emitted into the environment from anthropogenic sources such as combustion processes, vehicle emissions and industrial sources, as well as from biogenic processes [1,2]. Organic contaminants exist at very low concentrations in the water [3]. Therefore, it is essential that the organic contaminants be removed from the drinking water [4]. Natural purification of water systems such as rivers, creeks, lakes, and pools is realized by the solar light falling on the earth. Sunbeams initiate the degradation reaction of big organic molecules into smaller and basic molecules, finally providing for the formation of CO2, H2O and other molecules [5,6].

In its reactions with organic molecules, OH behaves as an electrophile whereas O is a nucleophile. Thus, OH readily adds to unsaturated bonds while O does not. Both forms of the radical abstract H from C-H bonds and this can result in the formation of different products when the pH is raised to a range where O rather than OH is the reactant. For example, if an aromatic molecule carries an aliphatic side chain, O attacks there by radical abstract H whilst OH adds preferentially to the aromatic ring [7]. The hydroxyl radical which is the most reactive type known in biological systems reacts with every biomolecule it encounters, including water. Potentially, every biomolecule is a hydroxyl radical scavenger at different speeds [8]. Aromatic compounds are good detectors since they hydroxylate. In addition, the position of attack to the ring depends on the electron withdrawal and the repulsion of previously present substituents. The attack of any hydroxyl radical to an aromatic compound results in the formation of a hydroxylated product [9]. Ortho-toluidine used as an intermediate in large volumes of herbicides can be solved little in water, yet can be solved in acohol, ether, and diluted acids. Toluidine is a synthetic chemical that is normally a light yellow liquid, but turns to a reddish brown when exposed to air and light [10]. The chemical properties of toluidine are very similar to aniline and it has common features with other aromatic amines. It is a weak basic due to the amino group that is attached to the aromatic ring.  At room temperature and pressure, ortho-and-meta-toluidines are viscous liquids; however the molecules in para-touidine are more symmetrical and fit the crystal structures [11, 12].

* To whom all correspondence should be sent:
E-mail: yyalcin@nku.edu.tr

While an intermediate in aminotoluene herbicide synthesis is used in the production of more than 90 paints and pigments, rubber, chemicals and pesticides, it is also used as a hardening agent for epoxy resin systems, a reactive material for glucose analysis and fibre dying in clinical laboratories [13]. Due to the damaging effects of living organisms emitting resistant foul smell and because of their solubility, aminotoluenes and their derivatives constitute an important water contaminant group. Although many methods are available for the removal of these molecules from water, every method has its own inconvenience [13-18].

In the study of Eren et al.[18] the most probable reaction paths of the aminotoluene (o-toluidine) molecule with OH radicals have been analyzed. The optimized geometry was calculated via Gauss View 5. Subsequently, the lowest energy level was found through geometric optimization via the Gaussian 09 programme. The geometrical structure analysis and bond lengths were also calculated. According to the DFT method the constant k and the entropy were found to be the highest, the enthalpy and Gibbs free energy values were the lowest, the transition states of ATnm, OATnm, MATnm, PATnm, NMATo and NMATm were concluded to be the most stable and had the lowest energy transition complexes [18].

In this study, the kinetics of the degradation reaction of the transition states of ATnm, OATnm, MATnm, PATnm, NMATo and NMATm and the hydroxyl derivatives were analyzed theoretically. With the aim to determine the intermediates obtained from the reaction of aminotoluene degradation, geometric optimization of the reactant and the transition state complexes were realized through AM1 and PM3, HF/3-21G, HF/6-31G* and DFT methods. Based on the quantum mechanical calculation, all the probable rate constants of the reaction paths were calculated by using TST.

## COMPUTATIONAL SET-UP AND METHODOLOGY

### *Computational models*

The molecular models were created by using the mean bond distances, the geometric parameters of the benzene ring, the tetrahedral angles for sp3-hybridized carbon and oxygen atoms and 1200 for the sp2-hybridized carbon atoms. In the calculation of the hydroxylated radicals, the aromatic ring was left planar except for the position of attack. The attacking •OH radical was assumed to form a tetrahedral angle with the C–H bond due to the

change in the hybridization state of the carbon at the addition centre from sp2 to sp3 [2,18].

### *Molecular Orbital Calculations*

It is possible that in the photocatalytic degradation reactions of organic contaminants, more harmful products may occur than in the original material. Therefore, before experimentally realizing a photocatalytic degradation reaction, it is essential to know what the primary intermediate products are. The most reliable and accurate information is gathered through calculations carried out with quantum mechanical methods. Thus, since the yield produced is the same, the photocatalytic degradation reaction of transition state complexes and their hydroxy derivatives is based on the direct reaction of these molecules with the OH radical. With this aim, the kinetics of the reactions of the complexes and complexes derivatives with OH radicals was theoretically analyzed. The study was initiated with complexes and then exposed to an OH radical reaction and the reaction of the yield was modelled at the gas phase. The experimental findings in the scientific literature show that OH radicals detach a hydrogen atom from the saturated hydrocarbons and OH is added to the unsaturated hydrocarbons and materials of the aromatic structure [18,19]. For this purpose, all the possible reaction paths for the analyzed reactions were determined, for every reaction path molecular orbital calculations of the reactant, yield and transition state complexes were carried out with the AM1, PM3, HF and DFT methods, their molecular orbital calculations were realized and their geometries were optimized.

### *Kinetic Data Treatment*

The aim of this study was to develop a model providing the outcome of the yield distribution of the photocatalytic degradation reactions. The vibration frequencies, the thermodynamic and electronic features of every structure were calculated using the obtained optimum geometric parameters. Afterwards, the rate constant and activation energy of every reaction was calculated using the Transition State Theory for a temperature of 25°C based on the quantum mechanical calculation results.

In order to find out the reaction rate, it is necessary to calculate the equilibrium constant. The equilibrium constant is calculated using the partition functions in accordance with the mechanical methods. If the equilibrium constant $K^{\neq}$ is written in terms of partition functions, it is as follows:

$$K^{\neq} = \frac{q^{\neq}}{q'_A q'_B} \quad , (1)$$

q#, qA, qB: partition functions belonging to the transition state complex and reactants. The molecular partition function is as given below:

$$q' = qe^{-Ea(RT)^{-1}} \quad , (2)$$

Ea represents the activation energy, the difference between the zero point energies of the transition state complex and the reactants [18,20].

$$k = \frac{k_B T}{h} \frac{q^{\neq}}{q_A q_B} e^{-Ea(RT)^{-1}} \quad , (3)$$

kB   : Boltzmann constant
h    : Planck constant
T    : absolute temperature

In order to be able to calculate the rate constant, it is necessary to initially calculate the partition function of the activated complex. To realize this calculation, it is essential to know the geometry of the complex and moments of inertia. In addition, Ea should be known in order to find out the rate constant. The activation energy like the vibration frequency can only be calculated quantum mechanically.

The most probable reaction path and yield distribution of the OH radical of every molecule was determined by comparing the obtained results. The optimized geometric structures were drawn via GaussView 5 and the calculations were done via the Gaussian 09 packet programme [18,21].

*Methodology*

Experimental studies were carried out recently for oxidative degradation mechanisms of aromatic pollutants and monitoring the intermediate products formed during degradation. Rapidly evolving computer technology has entered into the workspace of the chemist and it has become inevitable to support the experimental results with theoretical calculations. Methods widely used today for chemical purposes can be made more practical utilizing calculations in package software. Both methods for calculating molecular and electronic structures use the same calculations; namely they calculate the energy of a particular molecular structure and make the geometric optimization (find the lowest energy molecular structure and equilibrium geometry). Geometry optimizations are fundamentally based on the energy gradient that is the first derivative of the energy according to its position [22].

The reaction system under consideration consists of •OH radicals that are open-shell species. It is well-known that open-shell molecules pose severe problems in quantum mechanical calculations. Therefore, the geometry optimization of the reactants, the product radicals, pre-reactive and transition state complexes were performed by the AM1, PM3, HF and DFT methods with the Gaussian 09 package [18,21].

Electronic structure methods use the laws of quantum mechanics rather than the laws of classical physics. These methods are characterized by different approaches to the mathematical methods. The electronic structure methods, semiemprical methods and ab-initio methods are parts of two main groups. The AM1 and PM3 method are semiemprical methods that we use in this study. Ab-initio methods do not use experimental data except for the basic physical constants (speed of light, Planck's constant, the mass of the electron, ... etc) of the molecules of interest unlike the molecular mechanics and the semiempirical method. Only the valence electrons are taken into account in the calculation and the basic functions are defined by Slater-type orbitals [23].

DFT methods use the exact electron density to calculate the molecular properties and energies, taking the electron correlation into account. They do not suffer from spin contamination and this feature makes them suitable for calculations involving open-shell systems. The DFT calculations were carried out by the hybrid B3LYP functional, which combines HF and Becke exchange terms with the Lee–Yang–Parr correlation functional.

The choice of the basis set is very important in such calculations. Based on these results, optimizations in the present study were performed at the B3LYP/6-31G(d) level. Forming C–O bonds in the addition paths and the H–O bond in the abstraction path were chosen as the reaction coordinates in the determination of the transition states. Ground-state and transition-state structures were confirmed by frequency analyses at the same level. Transition structures were characterized by having one imaginary frequency that belonged to the reaction coordinate, corresponding to a first-order saddle point. Zero-point vibrational energies (ZPEs) were calculated at the B3LYP/6-31G(d) level [2,18].

In recent years, the density functional theory (DFT) based on these methods has become very popular. The best DFT method requires less computing power than the conventional correlation method. This method is widely preferred for systems with too many atoms and makes calculations for a shorter time compared to other ab-initio methods. Generally, such ab-initio or DFT

is used to create the initial structure for the optimization in large systems. It used to obtain the qualitative information such as molecular orbitals, atomic loads and vibrational modes of a molecule and to predict the energy on conformation and substituent effects [22].

### Solvent effect model

In aqueous media, water molecules affect the energetics of the degradation reactions of all organic compounds. Moreover, $H_2O$ induces geometry relaxation on the solutes. The latter effect becomes more important when hydrogen-bonded complexes are present. However, the results obtained in earlier studies indicate that geometry changes have a negligible effect on the energy of the solute in water for both open- and closed-shell structures [18,24,25]. In this study, to take into account the effect of $H_2O$ on the energetics and the kinetics of the aminotoluene + •OH reactions, DFT/B3LYP/6-31+G(d) calculations were carried out for the optimized structures of the reactants, the pre-reactive and the transition state complexes and the product radicals, by using COSMO (conductor-like screening solvation model) [18,25] as the solvation model, implemented in the Gaussian 09 package. The solvent was water at 25°C, with a dielectric constant $\varepsilon = 78.39$ [18,22].

COSMO is one of the polarizable continuum methods (PCMs). In PCMs, the solute molecule is placed in a cavity surrounded by a polarizable continuum, whose reaction field modifies the energy and the properties of the solute [18,26]. The geometry of the cavity is determined by the shape of the solute. The reaction field is described in terms of the apparent polarization charges or reaction field factors included in the solute Hamiltonian, so that it is possible to perform iterative procedures leading to self-consistence between the solute wave-function and the solvent polarization. The COSMO method describes the solvent reaction field by means of apparent polarization charges distributed on the cavity surface, which are determined by assuming that the total electrostatic potential cancels out at the surface. This condition can describe the solvation in polar liquids. Hence, it is the method of choice in this study [2,18].
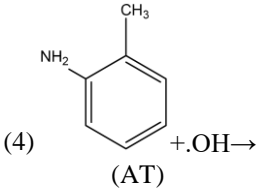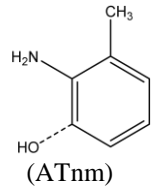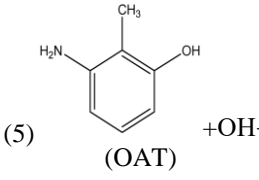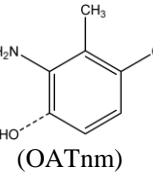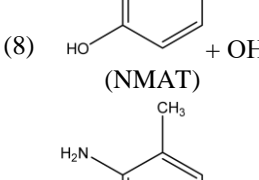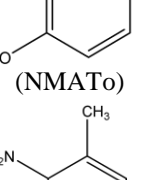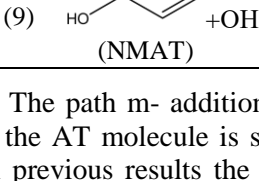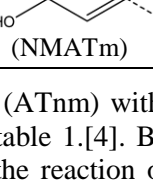
### RESULTS AND DISCUSSION
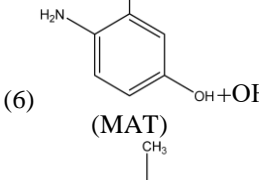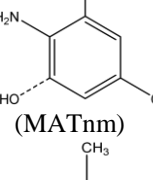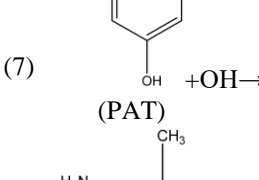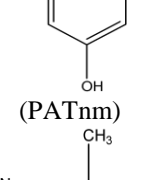
#### Computational modelling

#### Reaction paths

The hydroxyl radical is a very active species and has a strong electrophilic character. [18,27]. Once

formed, it can readily attack the aminotoluene molecule and produce the reaction intermediates. •OH radical reactions with aromatic compounds proceed through the following reaction pathway: H-atom abstraction from C–H bonds and addition to aromatic rings.18,28 Based on previous results the 6,7,8,9,18,19,29 path for the reaction of aminotoluene(AT) with •OH was determined.

**Table 1.** The reaction paths of the most stable TST complexes of AT with .OH.

| OH addition | TST |
|---|---|
| (4) (AT) +.OH→ | (ATnm) |
| (5) (OAT) +OH→ | (OATnm) |
| (6) (MAT) +OH→ | (MATnm) |
| (7) (PAT) +OH→ | (PATnm) |
| (8) (NMAT) + OH→ | (NMATo) |
| (9) (NMAT) +OH→ | (NMATm) |

The path m- addition to NH2 (ATnm) with TS to the AT molecule is shown in table 1.[4]. Based on previous results the path for the reaction of 3-hydroxy-2- methyl aniline (OAT) with •OH was determined. The path m- addition to NH2 (OATnm) with TS to a OAT molecule is shown

table 1.(5). Based on previous results the path for the reaction of 4-hydroxy-2- methyl aniline (MAT) with •OH was determined. The path m-addition to NH2 (MATnm) with TS to a MAT molecule is shown in table 1.[6].

Based on previous results the path for the reaction of 5-hydroxy-2- methyl aniline (PAT) with •OH was determined. The path m- addition to NH2 (PATnm) with TS to a PAT molecule is shown in table 1.(7). Based on previous results two different paths for the reaction of 2-hydroxy-6- methyl aniline (NMAT) with •OH were determined. The first two paths, o-addition (NMATo) and m-addition (NMATm) with TS to a NMAT molecule are shown in table 1. [8.9].
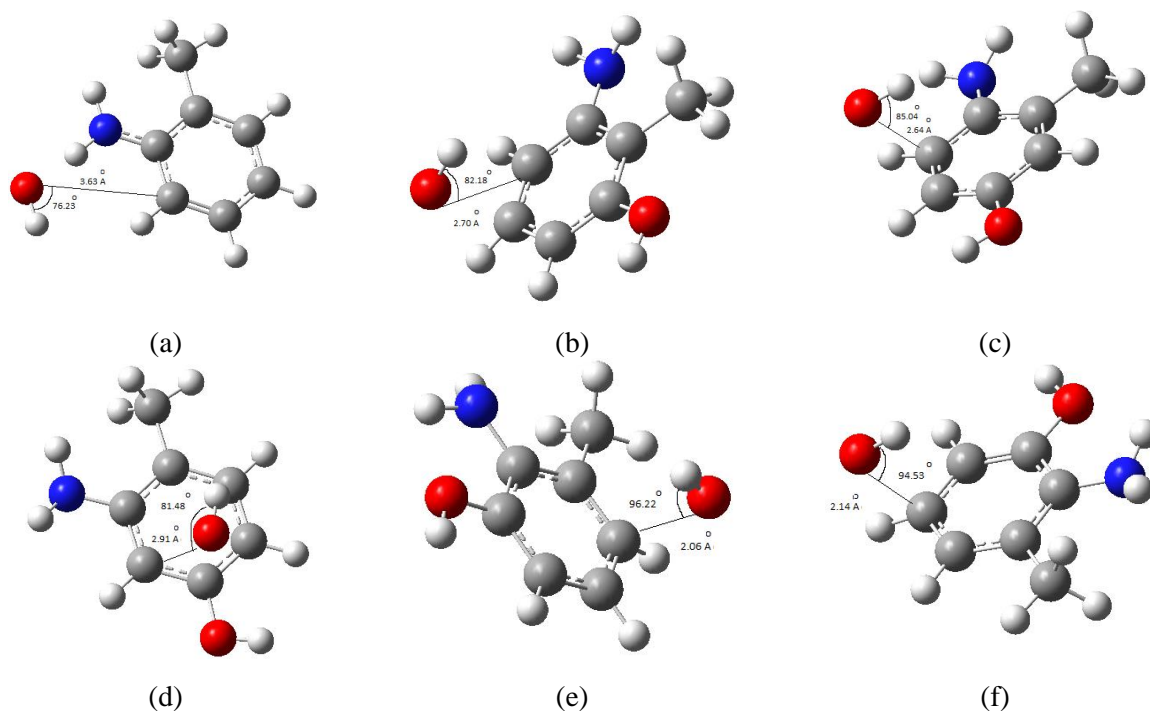
### Transition State Complexes

In this study, reactants were used to find out the transition state complexes. An estimation of the initial geometry was done according to the type of reaction path using the optimum geometric parameters of the reactants. A C-O bond was chosen as the reaction coordinate while modelling the transition state complexes for the reactions realized with OH addition and the bond length was changed as 1.850-2.500 Å during calculation. The emerging OH bond length was chosen as the reaction path, and in order to determine the position of the OH radical according to the molecule, the dihedral angles belonging to this group were changed during the calculations. The activation energies and their most determined state in

thermodynamic terms for the gas phase and aqueous media were calculated for the probable reaction paths of all transition state complexes [18].

According to Fig.1, the C-O bond lengths at four probable transition states of the OH radical were taken as precise measurements. The bond lengths were calculated as (a) ATnm (3.63 Å), (b) OATnm (2.70 Å), (c) MATnm (2.64 Å), (d) PATnm (2.91 Å), (e) NMATo (2.06 Å), (f) NMATm (2.14 Å) relatively. The longest C-O bond belongs to the ATnm TS molecule and it is found that it occurs later compared to the others. Therefore, it is the most probable transition state.

### CONCLUSIONS

It is possible that much more harmful intermediates than the ones at the beginning may occur given photocatalytic reactions of organic pollutants. The primary substances of such organic pollutants are polyaromatic substances. Thus, before realizing the photocatalytic degradation reaction experimentally, it is essential to know what the primary intermediates are. This information gives the most reliable and accurate calculations made by the quantum mechanical methods. Therefore, since the final product is the same, the photocatalytic degradation reaction of the transition state complexes and hydroxy derivatives are both based on the direct reaction with the OH radical of the transition state complexes.



(a)  (b)  (c)

(d)  (e)  (f)

**Fig. 1.** Optimized structures of the transition state complexes of probable reaction paths (4-9): **(a)** ATnm, (b) OATnm, (c) MATnm, (d) PATnm, (e) NMATo, (f) NMATm

**Table2.** According to the DFT method the constant k, entropy, enthalpy and Gibbs free energy values.[18].

| DFT | $\Delta H(10^2)$ (kcal mol$^{-1}$) | $\Delta G(10^2)$ (kcal mol$^{-1}$) | $\Delta S$ (kcal mol$^{-1}$ K$^{-1}$) | k | $\Delta E (10^2)$ (kcal mol$^{-1}$) |
|---|---|---|---|---|---|
| AT | 0.964 | 0.718 | 0.082 | -------- | 0.958 |
| ATo | 1.047 | 0.765 | 0.095 | $1.145 \times 10^{11}$ | 1.041 |
| ATm | 1.042 | 0.749 | 0.098 | $3.738 \times 10^{8}$ | 1.036 |
| ATp | 1.046 | 0.764 | 0.094 | $1.568 \times 10^{9}$ | 1.040 |
| ATnm | 1.033 | 0.747 | 0.096 | $2.257 \times 10^{12}$ | 1.028 |
| | | | | | |
| OAT | 0.998 | 0.735 | 0.088 | -------- | 0.992 |
| OATm | 1.084 | 0.798 | 0.096 | $6.028 \times 10^{15}$ | 1.078 |
| OATp | 1.079 | 0.779 | 0.101 | $1.376 \times 10^{9}$ | 1.073 |
| OATnm | 1.079 | 0.778 | 0.101 | $1.005 \times 10^{9}$ | 1.073 |
| | | | | | |
| MAT | 0.997 | 0.733 | 0.089 | --------- | 0.991 |
| MATo | 1.078 | 0.777 | 0.101 | $2.386 \times 10^{10}$ | 1.072 |
| MATp | 1.079 | 0.779 | 0.101 | $1.905 \times 10^{10}$ | 1.073 |
| MATnm | 1.076 | 0.772 | 0.102 | $9.504 \times 10^{4}$ | 1.070 |
| | | | | | |
| PAT | 0.997 | 0.735 | 0.088 | -------- | 0.991 |
| PATo | 1.072 | 0.775 | 0.100 | 0.000 | 1.066 |
| PATm | 1.083 | 0.798 | 0.096 | $4.015 \times 10^{15}$ | 1.077 |
| PATnm | 1.075 | 0.769 | 0.103 | $1.139 \times 10^{10}$ | 1.069 |
| | | | | | |
| NMAT | 0.998 | 0.735 | 0.088 | -------- | 0.992 |
| NMATo | 1.080 | 0.781 | 0.101 | $5.070 \times 10^{10}$ | 1.074 |
| NMATm | 1.080 | 0.778 | 0.101 | $2.505 \times 10^{11}$ | 1.074 |

In Table 2, according to the DFT method, the constant k and entropy have the highest values, the enthalpy and Gibbs free energy values are the lowest, the transition state of ATnm, OATnm, MATnm, PATnm, NMATo and NMATm are concluded to be the most stable and have the lowest energy transition of the complexes [18].

In this study, the analysis of the reaction kinetics of the most stable transition state complexes of the aminotoluene molecule by the theoretical methods was calculated. The DFT method is the most appropriate method of the theoretical methods used. The basic principle of DFT, is that the total electronic energy of the molecule is formed in connection with the total electronic density. Compared to other methods, this gives more accurate results that account for all the properties of the nucleus and electrons.

In Table 3, the activation energy levels of Ea in the gas phase of the TS molecules having the lowest energy for the DFT method for every transition state complex are given below: -7.404 kcal mol$^{-1}$ of ATnm for AT, -3.077 kcal mol$^{-1}$ of OATm for OAT, -5.131 kcal mol$^{-1}$ of MATnm for MAT, -4.049 kcal mol$^{-1}$ of PATnm for PAT, -5.402 kcal mol$^{-1}$ of NMATo for NMAT and -6.359 kcal mol$^{-1}$ of NMATm for NMAT are the transition state complexes with the lowest energy. These reveal the most probable transition state complexes in the gas phase. The most rapid occurring transition state complex in the gas phase has the highest values of the k rate constant. Ea$_{ecosmo}$ aqueous media activation energy levels for the DFT method at $1.927 \times 10^{1}$ kcal mol$^{-1}$ of ATnm for AT, $1.856 \times 10^{2}$ kcal mol$^{-1}$ of OATnm for OAT, $0.673 \times 10^{1}$ kcal mol$^{-1}$ of MATnm for MAT, $0.763 \times 10^{1}$ kcal mol$^{-1}$ of PATnm for PAT, $0.210 \times 10^{1}$ kcal mol$^{-1}$ of NMATo for NMAT and $0.607 \times 10^{1}$ kcal mol$^{-1}$ of NMATm for NMAT are the transition state complexes with the lowest energy.

This reveals that it is the most probable transition state at aqueous media. Hydroxyl radicals are used in order to remove the organic contaminants from water. In this study, the most probable reaction paths were determined to be OH radicals added to the aromatic ring.

Organic contaminants exist at very low concentrations in water [3,18]. Therefore, it is essential to remove the organic contaminants from the drinking water [4,18]. The hydroxyl radical, which is the most reactive type known in biological systems, reacts with every biomolecule it encounters including water. Potentially, every biomolecule is a hydroxyl radical scavenger at a different speed [8,18].

**Table 3.** Constant k, for gas phase and aqueous media activation energy levels calculated via AM1, PM3, HF, DFT methods

| ATnm | Ea(kcal mol$^{-1}$) | k | Ea$_{ecosmo}$(kcal mol$^{-1}$) |
|---|---|---|---|
| AM1 | -1.671 | $1.280 \times 10^8$ | $2.146 \times 10^1$ |
| PM3 | 1.634 | $2.729 \times 10^5$ | $2.770 \times 10^1$ |
| HF3 | 5.833 | $1.227 \times 10^2$ | $3.749 \times 10^1$ |
| HF6 | 8.494 | 1.794 | $4.493 \times 10^1$ |
| DFT | -7.404 | $2.257 \times 10^{12}$ | $1.927 \times 10^1$ |
| OATnm | Ea(kcal mol$^{-1}$) | k | Ea$_{ecosmo}$(kcal mol$^{-1}$) |
| AM1 | 0.337 | $6.805 \times 10^6$ | $2.165 \times 10^2$ |
| PM3 | 2.922 | $4.969 \times 10^4$ | $1.835 \times 10^2$ |
| HF3 | $1.055 \times 10^1$ | 0.070 | $2.196 \times 10^2$ |
| HF6 | $1.251 \times 10^1$ | $2.687 \times 10^{-3}$ | $2.140 \times 10^2$ |
| DFT | -3.077 | $1.005 \times 10^9$ | $1.856 \times 10^2$ |
| MATnm | Ea(kcal mol$^{-1}$) | k | Ea$_{ecosmo}$(kcal mol$^{-1}$) |
| AM1 | 0.808 | $1.742 \times 10^6$ | $0.864 \times 10^1$ |
| PM3 | 2.200 | $2.607 \times 10^5$ | $1.039 \times 10^1$ |
| HF3 | 5.522 | $6.091 \times 10$ | $1.921 \times 10^1$ |
| HF6 | 9.463 | 0.401 | $2.499 \times 10^1$ |
| DFT | -5.131 | $9.504 \times 10^4$ | $0.673 \times 10^1$ |
| PATnm | Ea(kcal mol$^{-1}$) | k | Ea$_{ecosmo}$(kcal mol$^{-1}$) |
| AM1 | -2.015 | $2.246 \times 10^8$ | $0.962 \times 10^1$ |
| PM3 | 2.304 | $2.116 \times 10^5$ | $1.132 \times 10^1$ |
| HF3 | 8.631 | 1.438 | $2.078 \times 10^1$ |
| HF6 | $1.016 \times 10^1$ | 0.117 | $2.634 \times 10^1$ |
| DFT | -4.049 | $1.139 \times 10^{10}$ | $0.763 \times 10^1$ |
| NMATo | Ea(kcal mol$^{-1}$) | k | Ea$_{ecosmo}$(kcal mol$^{-1}$) |
| AM1 | -0.605 | $2.707 \times 10^7$ | $0.731 \times 10^1$ |
| PM3 | 2.619 | $1.171 \times 10^5$ | $0.702 \times 10^1$ |
| HF3 | -2.222 | $1.075 \times 10^9$ | $1.298 \times 10^1$ |
| HF6 | $1.059 \times 10^1$ | 0.072 | $1.840 \times 10^1$ |
| DFT | -5.402 | $5.070 \times 10^{10}$ | $0.210 \times 10^1$ |
| NMATm | Ea(kcal mol$^{-1}$) | k | Ea$_{ecosmo}$(kcal mol$^{-1}$) |
| AM1 | -1.698 | $1.954 \times 10^8$ | $0.413 \times 10^1$ |
| PM3 | 2.475 | $1.744 \times 10^5$ | $0.665 \times 10^1$ |
| HF3 | 7.262 | $1.165 \times 10^1$ | $1.867 \times 10^1$ |
| HF6 | $1.015 \times 10^1$ | 0.110 | $2.365 \times 10^1$ |
| DFT | -6.359 | $2.505 \times 10^{11}$ | $0.607 \times 10^1$ |

**Table 4.** Mulliken loads of the heavy atoms of the studied molecules.[18]

| AT | ATnm | OAT | OAT nm |
|---|---|---|---|
| 11 C  -0.079158 | 11 C  -0.063830 | 10 C  -0.062126 | 10 C  -0.041225 |
| 15 N  -0.152651 | 15 N  -0.068889 | 14 N  -0.151131 | 14 N  -0.145082 |
|  | 18 O  -0.231787 | 17 O  -0.246327 | 17 O  -0.240589 |
|  |  |  | 19 O  -0.211082 |
| MAT | MATnm | PAT | PATnm |
| 10 O  -0.253210 | 10 O  -0.243592 | 10 C  -0.086504 | 10 C  -0.074263 |
| 12 N  -0.160178 | 12 N  -0.150491 | 14 N  -0.152124 | 14 N  -0.144674 |
| 15 C  -0.074152 | 15 C  -0.063696 | 17 O  -0.245155 | 17 O  -0.229721 |
|  | 19 O  -0.097024 |  | 19 O  -0.097927 |
| NMAT | NMATo | NMATm | |
| 10 C  -0.076104 | 10 C  -0.050241 | 10 C  -0.066739 | |
| 14 O  -0.262806 | 14 O  -0.239830 | 14 O  -0.256092 | |
| 16 N  -0.141021 | 16 N  -0.133101 | 16 N  -0.114022 | |
|  | 19 O  -0.220675 | 19 O  -0.223159 | |

Aromatic compounds are good detectors since they hydroxylate. In addition, the position of attack to the ring depends on the electron withdrawal and repulsion of the previously present substituents [9,18]. When the mulliken loads in table 4 are analyzed, the electronegativities of the N and O atoms yield information about the bonding state of the OH radical.

REFERENCES

1. B.J. Finlayson-Pitts, J.N. Pitts Jr., Chemistry of the Upper and Lower Atmosphere, Academic Press, San Diego, 2000.
2. A. Hatipoglu, D. Vione, Y. Yalçın, C. Minero, Z. Çınar, *Journal of Photochemistry and Photobiology A: Chemistry*, **215**, 59 (2010).
3. K. Verschueren, "Handbook of Environmental Data on Organic Chemicals" Second Ed., Van Nostrand Reinhold Company, New York, 1983.
4. J. C. English, V. S. Bhat, G. L. Ball, C. J. McLellan, O*riginal Research Article Regulatory Toxicology and Pharmacology,* **64**, 2, 269 (2012).
5. R.W. Matthews, D.F. Ollis, H. Al-Ekabi, Photocatalytic Purification and Treatment of Water and Air:in, Elsevier Sciense Publishers, 1993, p. 121.
6. *6. A.* Taicheng, L. Sun, G. Li, S. Wan, *Journal of Molecular Catalysis A:Chemical,* **333**(1–2), 128 (2010).
7. *7.* V.G. Buxton, L.C. Greenstock, P.W. Helman, B.A. Ross, *Journal of Physical and Chemical Reference Data*, **17**, 513 (1988).
8. 8. M. Anbar, P. Neta, *Int. J. Radiat Isot*, **18**, 495 (1965).
9. B. Halliwell, M. Grootveld, J.M.C. Gutteridge, 1988, Methods of Bıochemical Analysis, 33, 59. Laidler K.J and Meiser, J.H, Physical Chemistry, The Benjamin/Cummings Publishing Company Inc., California, 1982.
10. M J. O'Neil, Whitehouse Station, NJ: Merck & Co. Inc.*:* The Merck Index, 14ᵗʰ ed.; Editor, O'Neil M J., 2006, p. 1639.
11. C. Alba-Simionesco, J. Fan, C.A. Angell, *J. Chem. Phys.* **110**, 5262, (1999).
12. G. Pratesi, P. Bartolini, D. Senatra, M. Ricci, R. Righini, F. Barocchi, R. Torre. *Physical Review E :* **67**, 021505 (2003).
13. *IARC Monogr Eval Carcinog Risks Hum,* **99**, 1 (2010). PMID:21528837
14. *IARC Monogr Eval Carcinog Risk Chem Man*, **16**, 1 (1978).
15. *IARC Monogr Eval Carcinog Risks Chem Hum*, **27**, 1 (1982). PMID:6955259
16. *IARC Monogr Eval Carcinog Risks Hum Suppl,* **7**, 1 (1987). PMID:3482203
17. *IARC Monogr Eval Carcinog Risks Hum*, **77,** 1 (2000). PMID:11236796
18. B. Eren, Y.Yalcin Gurkan, *Bulg. Chem. Commun.* **47**(3), 849, (2015).
19. P.W. Atkins, Physical Chemistry, 6th edition, Oxford University Press, 1998, P.W. Atkins, R.S. Friedman, Molecular Quantum Mechanics, 3rd Ed., Oxford Univertsity Press Inc., New York, 1997.
20. I.N. Levine Quantum Chemistry, Allyn and Bacon Inc., Boston 1983, I.N. Levine, Quantum Chemistry i, Allyn and Bacon, Boston MA, 1991, J.P. Lowe, Quantum Chemistry, 2nd Ed., Academic Press, USA 1993.
21. 21. M.J. Frisch, G.W. Trucks, H.B. Schlegel, G.E. Scuseria, M.A. Robb, J.R. Cheeseman, J.A. Montgomery Jr., T. Vreven, K.N. Kudin, J.C. Burant, J.M. Millam, S.S. Iyengar, J. Tomasi, V. Barone, B. Mennucci, M. Cossi, G. Scalmani, N. Rega, G.A. Petersson, H. Nakatsuji, M. Hada, M. Ehara, K. Toyota, R. Fukuda, J. Hasegawa, M. Ishida, T. Nakajima, Y. Honda, O. Kitao, H. Nakai, M. Klene, X. Li, J.E. Knox, H.P. Hratchian, J.B. Cross, C. Adamo, J. Jaramillo, R. Gomperts, R.E. Stratmann, O. Yazyev, A.J. Austin, R. Cammi, C. Pomelli, J.W. Ochterski, P.Y. Ayala, K. Morokuma, G.A. Voth, P. Salvador, J.J. Dannenberg, V.G. Zakrzewski, S. Dapprich, A.D. Daniels, M.C. Strain, O. Farkas, D.K. Malick, A.D. Rabuck, K. Raghavachari, J.B. Foresman, J.V. Ortiz, Q. Cui, A.G. Baboul, S. Clifford, J. Cioslowski, B.B. Stefanov, G. Liu, A. Liashenko, P. Piskorz, I. Komaromi, R.L. Martin, D.J. Fox, T. Keith, M.A. Al-Laham, C.Y. Peng, A. Nanayakkara, M. Challacombe, P.M.W. Gill, B. Johnson, W. Chen, M.W. Wong, C. Gonzalez, J.A. Pople, Gaussian 09, Revision B.04, Gaussian, Inc., Pittsburgh, PA, 2009.
22. J.B. Foresman, Æ. Frisch, Exploring Chemistry with Electronic Structure Methods, Gaussian Inc., Pittsburgh, PA, 1996.
23. P. Popelier, Pearson Education: Atom in Molecules, USA, 2000.
24. J. Andzelm, C. Kölmel, A. Klamt, *J. Chem. Phys.* **103**, 9312 (1995).
25. V. Barone, M. Cossi, *J. Phys. Chem. A.*, **102,** 11 (1998).
26. N.S. Hush, J. Schamberger, G.B. Bacskay, *Coord. Chem. Rev.* **249**, 299, (2005).
27. V. Brezová, M. Ceppan, E. Brandsteterova, M. Breza, L. Lapcik, *J. Photochem. Photobiol. A: Chem.* **59**, 3 (1991).
28. M. Kılıc¸ G. Kocturk, N. San, Z. Çınar, *Chemosphere,* **69**, 9, 1396 (2007).
29. I. Suh, D. Zhang, R. Zhang, L.T. Molina, M.J. Molina, *Chem. Phys. Lett.* **364**, 454 (2002). .

# НАЙ-СТАБИЛНИТЕ ПРЕХОДНИ СЪСТОЯНИЯ НА МОЛЕКУЛАТА НА АМИНО-ТОЛУЕНА

Б. Ерен[1], Й.Й. Гуркан[2]*

[1]*Университет „Намик Кемал“, Факултет по земеделие, Текирдаг, Турция*
[21]*Университет „Намик Кемал“, Департамент по химия, Текирдаг, Турция*

(Резюме)

В тази работа са анализирани най-вероятните маршрути за преходните състояния ATnm, OATnm, MATnm, PATnm, NMATo и NMATm с OH-радикали. Оптимизираната геометрия на комплексите е определена чрез геометрична оптимизация с помощта на софтуера Gaussian 09. Анализът на геометричната структура и дължината на връзките също за изчислени. Тази работа има за цел да се определят най-вероятните пътища за разпределението на преходните комплекси и взаимодействията с OH-радикали в газова фаза и във водна среда. Използвани са квантово-механични методи за посочването на влиянието на скоростта на реакцията върху първичните, хидроксилираните междинни съединения и накрая – въздействието на разтворителя (водата). За определянето на междинните съединения при разлагането на преходните комплекси е използвана геометрична оптимизация с полу-емпирични методи (AM1 и PM3), *ab initio* Hartree-Fock HF/3-21G, HF/6-31G* и Density Functional Theory (DFT). Сравнени са и теоретично са оценени най-подходящия метод и неговата надеждност. Най-вероятните скоростни константи на реакционните пътища са изчислени с помощта на терията на преходните състояния (TST). За определянето на преходното състояние на реакцията е взета връзката C-O за база. Изчислена е активиращата енергия на вероятните реакции за всички преходни комплекси и най-стабилните им състояния от термодинамична гледна точка за газова фаза и течна среда. Изследвано е влиянието на водата като разтворител при използването на COSMO като солватационен модел.